Distribution, Characterization, and Genesis of Mordenite in Miocene Silicic Tuffs at Yucca Mountain, Nye County, Nevada

U.S. GEOLOGICAL SURVEY BULLETIN 1777

Prepared in cooperation with
U.S. Department of Energy

Distribution, Characterization, and Genesis of Mordenite in Miocene Silicic Tuffs at Yucca Mountain, Nye County, Nevada

By RICHARD A. SHEPPARD, ARTHUR J. GUDE, 3d, and JOAN J. FITZPATRICK

Prepared in cooperation with
U.S. Department of Energy

U.S. GEOLOGICAL SURVEY BULLETIN 1777

DEPARTMENT OF THE INTERIOR
DONALD PAUL HODEL, Secretary

U.S. GEOLOGICAL SURVEY
Dallas L. Peck, Director

UNITED STATES GOVERNMENT PRINTING OFFICE, WASHINGTON: 1988

For sale by the
Books and Open-File Reports Section
U.S. Geological Survey
Federal Center
Box 25425
Denver, CO 80225

Library of Congress Cataloging-in-Publication Data

Sheppard, Richard A.
Distribution, characterization, and genesis of mordenite in Miocene silicic tuffs at Yucca Mountain, Nye County, Nevada.

(U.S. Geological Survey bulletin ; 1777)
Bibliography: p.
Supt. of Docs. no.: I 19.3:1777
1. Mordenite—Nevada—Yucca Mountain Region. 2. Volcanic ash, tuff, etc.—Nevada—Yucca Mountain Region. 3. Geology, Stratigraphic—Miocene. 4. Geology—Nevada—Yucca Mountain Region. 5. Radioactive waste disposal in the ground—Nevada—Yucca Mountain Region. I. Gude, Arthur J. (Arthur James), 1917- . II. Fitzpatrick, Joan J. III. United States. Dept. of Energy. IV. Title. V. Series.
QE75.B9 no. 1777 557.3 s 87-600028
[QE391.M8] [621.48'38]

CONTENTS

FIGURES

TABLES

Distribution, Characterization, and Genesis of Mordenite in Miocene Silicic Tuffs at Yucca Mountain, Nye County, Nevada

By Richard A. Sheppard, Arthur J. Gude, 3d, *and* Joan J. Fitzpatrick

Abstract

Tuffs at Yucca Mountain in the southwestern Nevada volcanic field are being investigated as a possible deep repository for high-level radioactive wastes. A sequence, as much as about 3,000 meters thick, of Miocene silicic ash-flow tuffs, bedded tuffs, lavas, and flow breccias was derived chiefly from the Timber Mountain-Oasis Valley caldera complex. Previous studies by others of core from several drill holes have shown that much of the original vitric material of the volcanic and volcaniclastic rocks was altered during diagenesis to clay minerals, silica minerals, zeolites, and feldspars. Unaltered glass still persists in the upper part of the sequence, but zones characterized by clinoptilolite and mordenite, analcime, and albite follow in succession with depth.

Information on the distribution, characterization, and genesis of mordenite in selected samples of core from four drill holes was obtained by transmitted light microscopy, scanning electron microscopy, X-ray powder diffraction, and chemical analysis. In samples of tuff from the clinoptilolite-mordenite zone, mordenite makes up 0–90 percent of the tuff and is commonly associated with clinoptilolite. Pseudomorphs of mordenite after shards and pumice fragments are common. Mordenite occurs chiefly as a tangle of filiform crystals, as spherulites, and as layers of compact fibers. Individual mordenite crystals are <1–100 micrometers long and have length-to-width ratios of about 20–100. The mean index of refraction for the mordenite is 1.466–1.474, and the birefringence is low, about 0.003. Cell parameters show the following ranges: a=18.074–18.114 Å, b=20.435–20.528 Å, c=7.489–7.546 Å, and V=2,771–2,803 Å^3. Two new chemical analyses of relatively pure mordenite indicate Si:Al ratios of 4.78 and 5.06 and Na:K ratios of 2.19 and 0.57, respectively.

Where associated with clinoptilolite, the mordenite was formed earlier, later, or both earlier and later than the clinoptilolite. The chemical constitutents for some mordenite were derived from dissolution of the original silicic vitric material by ground water, but the constituents for some late-formed mordenite came from dissolution of clinoptilolite. Scanning electron microscopic examination shows the growth of filiform mordenite on partially dissolved clinoptilolite and is convincing textural evidence that diagenetic reactions formed mordenite at the expense of clinoptilolite. This is the first unequivocal evidence for this reaction in tuff at Yucca Mountain and the adjacent Nevada Test Site or, perhaps, anywhere else. Results of hydrothermal syntheses of mordenite from natural clinoptilolite by others indicate that formation of mordenite is favored by higher temperature, pH, or sodium ion concentration. At least some of the mordenite in the silicic tuffs beneath Yucca Mountain seems due to diagenesis in a relatively high thermal regime near the Timber Mountain caldera to the north.

INTRODUCTION

Yucca Mountain is located in southern Nevada, about 24 km east of the town of Beatty (fig. 1). The thick sequence of Miocene ash-flow tuffs beneath Yucca Mountain has been intensively studied from drill core since 1978 to determine its potential as an underground repository for high-level radioactive waste. These studies are part of the Nevada Nuclear Waste Storage Investigations Project, managed by the Nevada Operations Office of the Department of Energy. Mineralogical and petrological investigations of the tuffs are necessary for adequate characterization of the potential waste repository. Zeolites are common alteration minerals in the tuffs of Yucca Mountain, and could provide important natural barriers to the migration of certain radionuclides. In addition, the mineralogical and petrological studies provide information on the thermal and alteration history of the tuffs.

The mineralogical and petrological investigations of drill cores from Yucca Mountain have been undertaken chiefly by the Los Alamos National Laboratory, and

some of the results have been published by Sykes and others (1979), Bish (1981), Bish and others (1981, 1982), Caporuscio and others (1982), Vaniman and others (1984), and Carlos (1985). Our present study is restricted to cores from drill holes USW-G1, USW-G2, USW-G4, and UE25b-1H, and our investigations of the distribution, properties, and genesis of mordenite in the tuffs supplement other ongoing mineralogical studies at the Los Alamos National Laboratory.

Acknowledgments

We thank Richard W. Spengler for facilitating our sampling of core at the core library in Mercury, Nev., and for providing unpublished descriptions of the core. We greatly appreciate the guidance and patience James M. Nishi provided during our use of the scanning electron microscope. We also thank Barbara A. Lockett for preparing excellent thin sections from difficult materials.

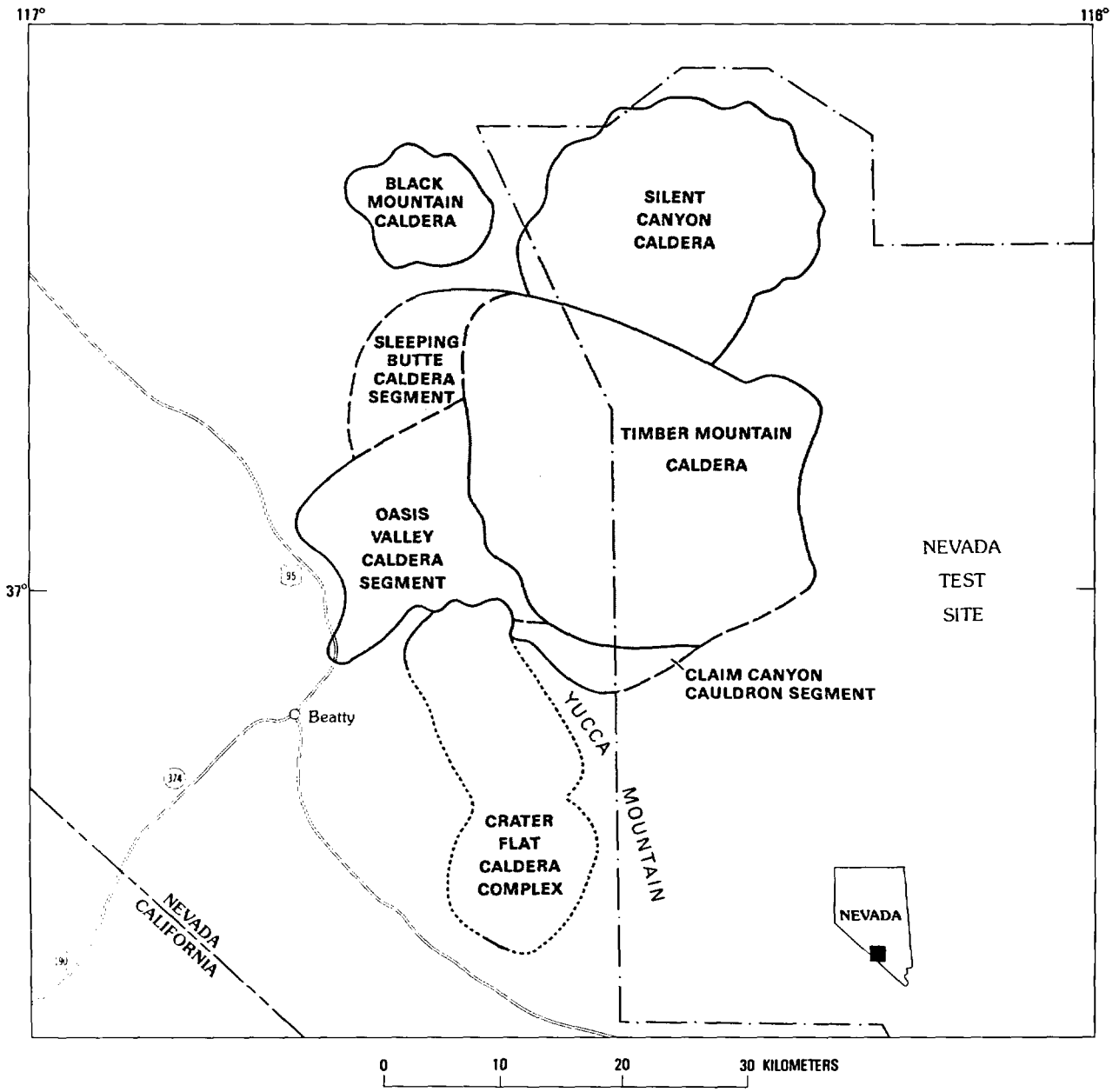

Figure 1. Location map showing Yucca Mountain, Nevada Test Site (NTS) boundary, and major calderas. Modified from Scott and Castellanos (1984).

Work was performed in cooperation with the U.S. Department of Energy for the Nevada Nuclear Waste Storage Investigations Project (Interagency Agreement DE-AI08-78ET44802).

GEOLOGIC SETTING

Yucca Mountain is within the southwestern Nevada volcanic field, which is a faulted, dissected volcanic plateau composed mainly of silicic ash-flow tuffs and minor lava flows and volcaniclastic rocks of Miocene age. Detailed geologic maps of Yucca Mountain and adjacent areas have been published by Christiansen and Lipman (1965), Lipman and McKay (1965), and Byers, Carr, Christiansen, and others (1976). Several calderas, including the Timber Mountain-Oasis Valley caldera complex, the Crater Flat caldera complex, the Tram caldera(?), and the Prow Pass and Bullfrog caldera(?) (Byers, Carr, Orkild, and others, 1976; Christiansen and others, 1977; Carr, 1982), lie just north and west of Yucca Mountain and are the sources for the volcanic rocks. Yucca Mountain consists of many north- to northwest-trending, eastward-tilted structural blocks that are repeated by westward-dipping, high-angle normal faults. The strata of Yucca Mountain dip mainly 5° -20° eastward.

A generalized geologic map of Yucca Mountain in the vicinity of the drill holes that will be discussed in this report is shown in figure 2. Except for remnants of the Timber Mountain Tuff, the exposed bedrock in the area of the drill holes is the Paintbrush Tuff. Stratigraphic units older than the Paintbrush Tuff crop out north of this area and occur in the subsurface at the drill hole sites. The core material used in our study came from drill holes USW-G2, USW-G1, USW-G4, and UE25b-1H, located from north to south. Drill holes USW-G3 and J-13 are located to the south of these four holes. Although cores from USW-G3 and J-13 were not sampled in our study, the distribution of mordenite in the tuffs of these two holes will be discussed briefly in the section, "Genesis of mordenite," in this report.

Stratigraphy

The general stratigraphy of the Miocene volcanic rocks penetrated by the drill holes at Yucca Mountain is summarized in table 1. The volcanic rocks are at least 1,830 m thick and perhaps as much as 3,050 m thick, and they range in age from 12.5 to 15.0 m.y. (Caporuscio and others, 1982). Detailed descriptions of the stratigraphy, lithology, and mineralogy of cores from the four drill holes have been given by Spengler and others (1979, 1981), Maldonado and Koether (1983), and Spengler and Chornack (1984). The Paintbrush Tuff is commonly the uppermost volcanic unit encountered in the holes, and consists, in descending order, of the Tiva Canyon, Yucca Mountain, Pah Canyon, and Topopah Spring Members. The Paintbrush Tuff consists chiefly of ash-flow tuffs that are moderately to densely welded and are devitrified. A densely welded, devitrified part of the Topopah Spring Member has received prime consideration as the host rock for a radioactive waste repository. The tuffaceous beds of Calico Hills underlie the Paintbrush Tuff and consist of a sequence of interbedded nonwelded, ash-flow tuffs and air-fall and reworked bedded tuffs. Beneath the tuffaceous beds of Calico Hills is the Crater Flat Tuff, which consists, in descending order, of the Prow Pass, Bullfrog, and Tram Members. The Crater Flat Tuff consists chiefly of ash-flow tuffs that are nonwelded to densely welded and locally devitrified. Relatively thin units of air-fall and reworked bedded tuff occur at the top and bottom of the Crater Flat Tuff and between the various members of the formation. Beneath the Crater Flat Tuff, in descending order, are an unnamed dacitic to rhyodacitic lava and flow breccia, the Lithic Ridge Tuff, and an older, unnamed sequence of ash-flow tuff, lava, flow breccia, and bedded tuff of rhyolitic to dacitic composition.

All stratigraphic units from the Pah Canyon Member of the Paintbrush Tuff down through the Lithic Ridge Tuff were sampled for our study. Because mineralogical studies by Bish and others (1982) had shown mordenite to be most abundant in the tuffaceous beds of Calico Hills and in the Crater Flat Tuff, we concentrated our sampling to core from these two units.

ANALYTICAL METHODS

The mineralogy of the core samples was determined by X-ray diffractometer analysis, using a Picker X-ray diffractometer (series 6240)[1]. Samples were first ground to a powder, and then packed in aluminum sample holders, exposed to copper radiation, and scanned at 2° 2θ per minute over the range of 2°-40° 2θ. Relative abundances of the minerals were visually estimated from the diffractometer patterns following the procedure outlined by Sheppard and Gude (1968, p. 2-3). Estimates are less reliable for samples containing glass or opal because these materials yield rather poor X-ray records. Unit-cell parameters for mordenite were determined by X-ray powder diffraction using a fully automated Siemens D-500 powder diffractometer equipped with a graphite monochromator that produced CuKα radiation. Data were collected over a range of 5°-70° 2θ at a step size of 0.02° 2θ and a count time of one second. Peak positions and cell parameters were refined using the algorithm of Appleman and Evans (1973) with constrained indexing.

[1]Any use of trade names in this report is for descriptive purposes only and does not imply endorsement by the U.S. Geological Survey.

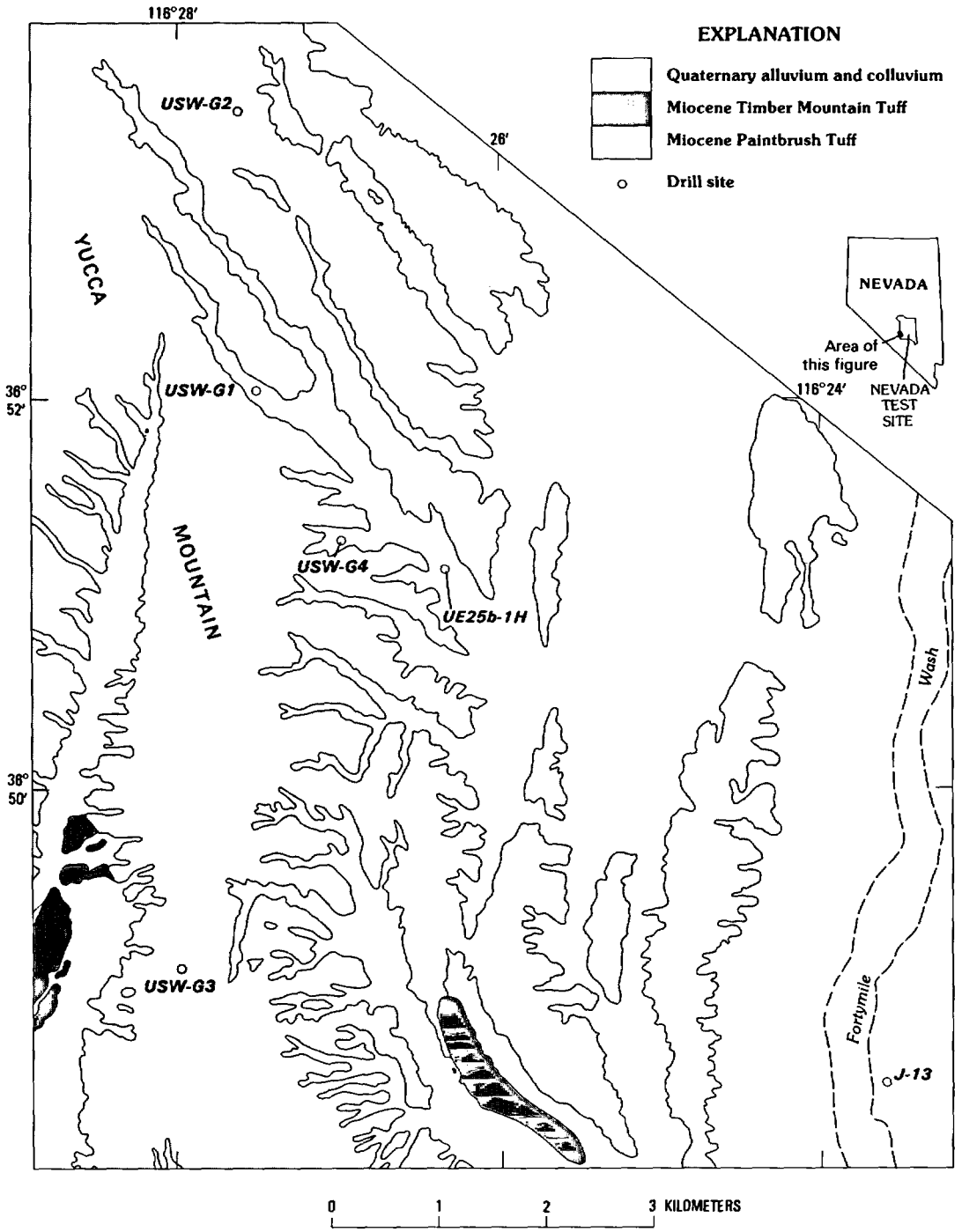

Figure 2. Generalized geologic map of Yucca Mountain in vicinity of the drill holes. Modified from Vaniman and others (1984).

Textures and paragenetic relationships of the diagenetic minerals were examined in thin sections of the core by transmitted-light petrographic microscopy and by scanning electron microscopy of freshly broken fragments of the core. A Cambridge Stereoscan 250 MK2 scanning electron microscope, equipped with a Tracor Northern energy dispersive X-ray unit, was used to study the fragments of core, which had been coated with a gold-palladium alloy.

The chemical compositions of bulk samples and mordenite separates were determined by standard X-ray fluorescence analyses. The H_2O content was determined by weight loss on ignition at 900 °C. The chemical composition of mordenite was also determined with an ARL

Table 1. Stratigraphy of Miocene volcanic rocks penetrated by drill holes at Yucca Mountain, Nevada
[Compiled from Spengler and others (1979, 1981), Maldonado and Koether (1983), and Spengler and Chornack (1984)]

Stratigraphic unit	Thickness (meters)	Description
Paintbrush Tuff		
Tiva Canyon Member	70-163	Ash-flow tuff; compound cooling unit of high-silica rhyolite to quartz latite; nonwelded base, but most is moderately to densely welded.
Yucca Mountain Member	0-30	Ash-flow tuff, rhyolitic, single cooling unit; nonwelded in upper and lower parts but moderately to densely welded in middle.
Unnamed tuff	0-47	Bedded and ash-flow tuff, nonwelded.
Pah Canyon Member	0-80	Ash-flow tuff, rhyolitic; single cooling unit having upper and lower nonwelded to slightly welded zones and a middle moderately to densely welded zone.
Topopah Spring Member	288-363	Ash-flow tuff, multiple; compound cooling unit; compositionally zoned from rhyolite to quartz latite; nonwelded upper and lower parts but moderately to densely welded middle.
Tuffaceous beds of Calico Hills	27-289	Ash-flow tuffs, rhyolitic, nonwelded; and numerous, thin, interbedded, reworked and ash-fall tuffs.
Crater Flat Tuff		
Prow Pass Member	82-193	Ash-flow tuff, rhyolitic; nonwelded to slightly welded upper and lower parts but moderately to densely welded middle; abundant lithic fragments of mudstone.

Table 1. Stratigraphy of Miocene volcanic rocks penetrated by drill holes at Yucca Mountain, Nevada—Continued

Stratigraphic unit	Thickness (meters)	Description
Bullfrog Member	89-193	Ash-flow tuff, rhyolitic; variable welding from nonwelded to densely welded.
Tram Member	154-372	Ash-flow tuff, rhyolitic; compound cooling unit with variable welding from nonwelded to densely welded; abundant lithic fragments of silicic volcanic rocks in upper part.
Unnamed dacite lava and flow breccia	0-249	Lava, flow breccia, and bedded tuff of rhyodacitic or dacitic composition.
Lithic Ridge Tuff	185-303	Ash-flow tuff, rhyolitic; single cooling unit; nonwelded to moderately welded; abundant lithic fragments of silicic volcanic rocks near middle.
Unnamed volcanic rocks and volcaniclastic sedimentary rocks	>345	Lava, flow breccia, ash-flow tuff, bedded ash-fall and reworked tuff, and conglomerate; rhyolitic, quartz latitic, and dacitic in composition.

electron microprobe on polished thin sections that had been coated with carbon.

DIAGENETIC MINERALOGY OF THE TUFFS

Hoover (1968) recognized and described a vertical zonation of diagenetic minerals in the Tertiary tuffs of the Nevada Test Site, north and east of Yucca Mountain. Based on mineralogical data from drill holes, tunnels, and outcrops, Hoover briefly described a downward succession of authigenic mineral assemblages characterized by glass, chabazite, clinoptilolite, mordenite, and then analcime. Later, Moncure and others (1981) delineated three vertical diagenetic zones in the Tertiary tuffs beneath Pahute Mesa in the northwestern part of the Nevada Test Site, north of Yucca Mountain. Based on mineralogical studies of drill core, Moncure and others (1981) demonstrated a downward succession of zones characterized by glass, clinoptilolite, and then analcime+albite. Actually, on the basis of the mineralogical descriptions provided by them (p. 388–389), the lowest zone could be subdivided into an upper analcime zone and a lower albite zone.

Preliminary petrologic studies of core from drill hole USW-G1 at Yucca Mountain led Bish and others (1981) to recognize four diagenetic zones in the silicic tuffs. These zones, named Zone I through Zone IV and adapted from Iijima (1978), are characterized downhole by glass, clinoptilolite + mordenite, analcime, and then albite, respectively. Subsequent mineralogical studies of all other drill holes in the silicic tuffs at Yucca Mountain recognized all or a portion of the same general diagenetic zonation.

The diagenetic mineral zonation for the four drill holes examined in our study is shown diagrammatically in figure 3. The four diagenetic zones were delineated on the basis of X-ray powder diffractometer data of bulk samples of core. Mineralogical data from more than 600 samples studied at the Los Alamos National Laboratory and about 100 additional samples (table 2) examined during our investigation were used to construct the diagram. The diagenetic zones are labeled with their characteristic mineral(s) and are the same vertical zones that have been recognized elsewhere beneath Yucca Mountain. We prefer to use the characteristic mineralogy to name the zones rather than Roman numerals (I–IV) as used previously by the Los Alamos National Laboratory because Iijima's (1978) use of numerals for zonal identification was originally applied to thick (commonly 3–6 km thick) marine sequences of silicic tuffs in Japan which are somewhat different from the terrigenous tuffs of Yucca Mountain, and because certain authigenic silicate minerals in the lower two zones in Japan have not been recognized beneath Yucca Mountain.

The zone boundaries shown in figure 3 were drawn at the first appearance in a downhole direction of a diagenetic mineral characteristic of the next lower zone. Thus, the top of the clinoptilolite-mordenite zone was placed at the first appearance of clinoptilolite or mordenite, the top of the analcime zone was placed at the first appearance of analcime, and the top of the albite zone was placed at the first appearance of albite. The zones vary in thickness and transgress stratigraphic boundaries, although the crosscutting relationships are not obvious in figure 3 because the members of the formations are not shown. The diagenetic zones rise in elevation from south to north, particularly between drill holes USW-G1 and USW-G2, a distance of only about 2.5 km.

In addition to the characteristic diagenetic mineral(s), each zone contains a variety of other diagenetic minerals as well as the original pyrogenic crystal (chiefly quartz, feldspars, and biotite) and lithic fragments. The glass zone commonly contains authigenic smectite and opal in addition to the glassy shards and pumice fragments. Associated authigenic minerals in the clinoptilolite-mordenite zone are opal and smectite or illite/smectite, and, locally in the lower part of the zone, authigenic quartz and potassium feldspar. The analcime zone commonly contains authigenic smectite or illite/smectite, quartz, potassium feldspar, and local relicts of clinoptilolite and mordenite. The albite zone commonly contains authigenic potassium feldspar, quartz, chlorite, and illite/smectite or illite as well as local relicts of analcime. Authigenic minerals that are common in shallower zones persist locally in the deeper zones. For example, clinoptilolite occurs in USW-G1 about 780 m beneath the top of the analcime zone (Bish and others, 1981).

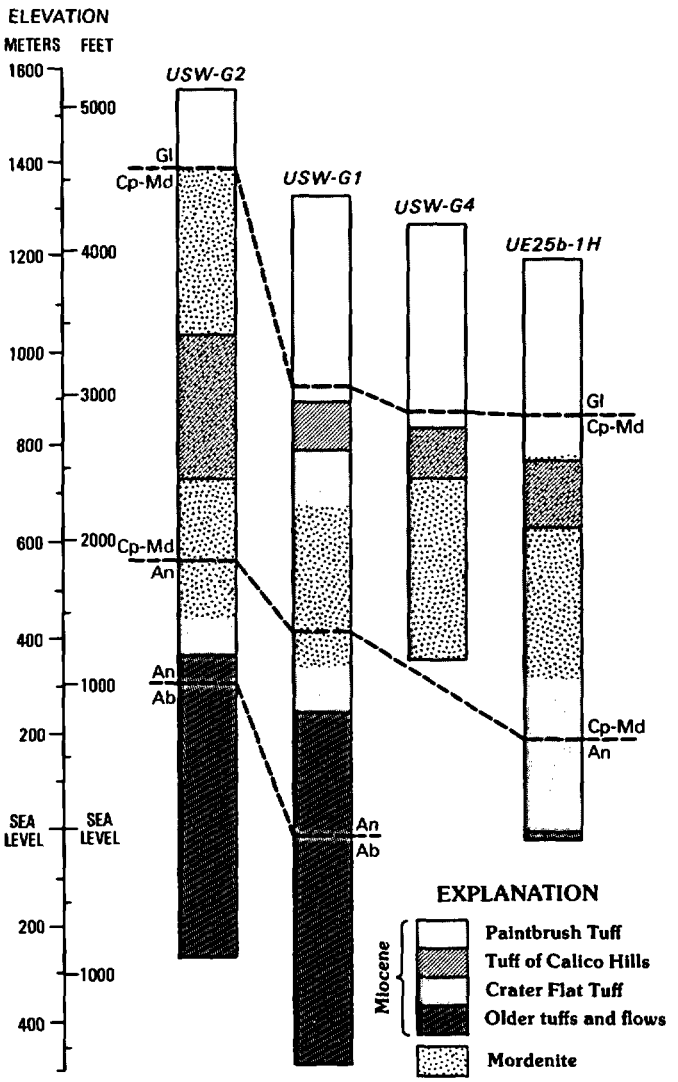

Figure 3. Diagram showing diagenetic zonation in drill holes USW-G2, USW-G1, USW-G4, and UE25b-1H. Drill holes are plotted elevation true and are arranged from north (left) to south (right). Dashed lines represent boundaries between the diagenetic zones, including glass (Gl), clinoptilolite-mordenite (Cp-Md), analcime (An), and albite (Ab).

Distribution of Mordenite

The distribution of mordenite in the four drill holes is shown diagrammatically in figure 3. Mordenite occurs chiefly in the Crater Flat Tuff and in the tuffaceous beds of Calico Hills, and ranges in abundance from trace amounts to more than 90 percent of the bulk tuff. The interval of mordenite-bearing tuff is thickest in drill hole USW-G2 where the mordenite occurs from the middle of the Pah Canyon Member of the Paintbrush Tuff downward to the upper part of the Tram Member of the Crater Flat Tuff, an interval of about 930 m. The magnitude of this mordenite-bearing interval in USW-G2 is

Table 2. Mineralogic composition of tuffs of Yucca Mountain, as estimated from X-ray diffractometer patterns of bulk samples of core

[---, looked for but not found; Tr, trace. Mica includes pyrogenic biotite and authigenic illite. Quartz includes pyrogenic and authigenic varieties. Traces of calcite identified in samples G1-3136.7, G1-4402.7, and UE25-2887.9. Sample number consists of two parts; abbreviated drill hole number preceding the dash and the depth (in feet to the nearest tenth of a foot) from which sample was collected following the dash. Stratigraphic units: Tpp, Pah Canyon Member of the Paintbrush Tuff; Tpt, Topopah Spring Member of the Paintbrush Tuff; Tht, tuffaceous beds of Calico Hills; Tcp, Prow Pass Member of the Crater Flat Tuff; Tcb, Bullfrog Member of the Crater Flat Tuff; Tct, Tram Member of the Crater Flat Tuff; Tlr, Lithic Ridge Tuff]

Sample No.	Stratigraphic unit	X-ray analysis (parts of ten)									
		Glass	Opal	Smectite	Mica	Clinoptilolite	Mordenite	Analcime	Alkali feldspar	Plagioclase	Quartz
Drill hole USW-G1											
G1-1300.0	Tpt	10	---	---	---	---	---	---	---	---	---
G1-1307.7	Tpt	10	---	---	---	---	---	---	---	Tr.	---
G1-1345.0	Tpt	10	---	---	---	---	---	---	---	Tr.	---
G1-1360.7	Tpt	10	---	Tr.	---	---	---	---	---	---	---
G1-1396.1	Tpt	10	---	Tr.	---	Tr.	---	---	---	---	---
G1-1409.9	Tpt	10	---	Tr.	---	Tr.	---	---	---	---	---
G1-1445.8	Tht	---	---	2	Tr.	8	---	---	---	---	Tr.
G1-2202.6	Tcb	---	2	Tr.	Tr.	5	---	---	3	---	Tr.
G1-2233.8	Tcb	---	1	Tr.	1	3	---	---	4	---	1
G1-2240.5	Tcb	---	Tr.	---	---	2	4	---	2	2	Tr.
G1-2257.2	Tcb	---	4	Tr.	---	Tr.	4	---	---	---	2
G1-2269.0	Tcb	---	---	---	---	1	9	---	---	---	---
G1-2291.1	Tcb	---	---	Tr.	---	Tr.	10	---	---	---	---
G1-2297.8	Tcb	---	---	---	---	10	Tr.	---	---	---	---
G1-3005.3	Tct	---	---	---	Tr.	---	---	Tr.	2	---	8

Table 2. Mineralogic composition of tuffs of Yucca Mountain, as estimated from X-ray diffractometer patterns of bulk samples of core—Continued

Sample No.	Stratigraphic unit	X-ray analysis (parts of ten)									
		Glass	Opal	Smectite	Mica	Clinoptilolite	Mordenite	Analcime	Alkali feldspar	Plagioclase	Quartz
Drill hole USW-G1											
G1-3029.5	Tct	---	---	---	Tr.	1	---	---	1	---	8
G1-3044.0	Tct	---	---	---	Tr.	4	---	---	3	---	3
G1-3073.4	Tct	---	---	---	---	1	---	Tr.	1	---	8
G1-3104.5	Tct	---	---	---	---	2	---	Tr.	2	---	6
G1-3114.1	Tct	---	---	---	Tr.	Tr.	---	1	2	---	7
G1-3136.7	Tct	---	---	2	Tr.	---	---	---	2	---	6
G1-3172.8	Tct	---	---	---	Tr.	---	Tr.	---	2	---	8
G1-3194.9	Tct	---	---	1	---	Tr.	1	---	2	---	6
G1-4306.6	Tlr	---	---	5	Tr.	---	---	Tr.	2	---	3
G1-4344.7	Tlr	---	---	7	---	---	---	Tr.	2	---	1
G1-4402.7	Tlr	---	---	5	---	---	---	Tr.	3	---	2
Drill hole USW-G2											
G2-551.6	Tpp	4	2	2	---	---	2	---	Tr.	Tr.	---
G2-560.5	Tpp	2	Tr.	1	---	Tr.	7	---	Tr.	---	---
G2-580.3	Tpp	1	---	Tr.	---	Tr.	8	---	1	---	---
G2-597.3	Tpp	5	---	---	---	---	5	---	Tr.	---	---
G2-616.7	Tpp	5	---	1	Tr.	---	4	---	Tr.	---	---
G2-631.0	Tpp	3	---	1	---	---	5	---	1	---	---
G2-641.9	Tpp	1	---	2	---	3	3	---	1	---	---
G2-649.7	Tpp	2	---	4	---	---	4	---	---	---	---
G2-1996.6	Tht	---	Tr.	1	---	Tr.	8	---	---	---	1
G2-2029.7	Tht	---	2	Tr.	---	4	3	---	---	---	1

Table 2. Mineralogic composition of tuffs of Yucca Mountain, as estimated from X-ray diffractometer patterns of bulk samples of core—Continued

Sample No.	Stratigraphic unit	X-ray analysis (parts of ten)									
		Glass	Opal	Smectite	Mica	Clinoptilolite	Mordenite	Analcime	Alkali feldspar	Plagioclase	Quartz
Drill hole USW-G2											
G2-2049.6	Tht	---	---	---	---	2	8	---	---	---	---
G2-2072.9	Tht	---	3	Tr.	---	2	5	---	Tr.	---	---
G2-2090.3	Tht	---	1	---	---	---	6	---	1	---	2
G2-2121.7	Tht	---	---	2	---	6	2	---	---	---	---
G2-2137.5	Tht	---	4	Tr.	---	---	6	---	---	---	---
G2-2156.7	Tht	---	2	---	---	2	6	---	---	---	---
G2-2204.0	Tht	---	2	---	---	---	8	---	---	---	---
G2-3192.2	Tcp	---	---	---	---	2	---	---	6	---	2
G2-3228.2	Tcp	---	---	1	---	---	Tr.	3	2	---	4
G2-3249.8	Tcp	---	---	Tr.	---	---	Tr.	6	1	---	3
G2-3259.0	Tcp	---	---	Tr.	---	---	---	1	2	---	7
G2-3275.6	Tcp	---	---	Tr.	---	---	2	Tr.	2	---	6
G2-3322.4	Tcb	---	---	---	Tr.	---	Tr.	---	4	---	6
G2-3358.0	Tcb	---	---	---	Tr.	---	---	---	2	---	8
G2-3383.9	Tcb	---	---	---	---	---	---	---	4	---	6
G2-3409.4	Tcb	---	---	---	---	---	---	---	3	---	7
G2-3454.6	Tcb	---	---	2	---	---	2	---	3	---	3
G2-3493.1	Tcb	---	---	---	---	---	3	---	---	---	7

Table 2. *Mineralogic composition of tuffs of Yucca Mountain, as estimated from X-ray diffractometer patterns of bulk samples of core—Continued*

Sample No.	Stratigraphic unit	X-ray analysis (parts of ten)									
		Glass	Opal	Smectite	Mica	Clinoptilolite	Mordenite	Analcime	Alkali feldspar	Plagioclase	Quartz
Drill hole USW-G4											
G4-1506.4	Tht	---	---	Tr.	---	10	---	---	---	---	---
G4-1531.8	Tht	---	---	---	---	10	Tr.	---	---	---	---
G4-1546.3	Tht	---	---	Tr.	---	8	2	---	---	---	---
G4-1561.2	Tht	---	---	Tr.	---	9	---	---	1	---	---
G4-1584.6	Tht	---	---	Tr.	---	6	4	---	---	---	---
G4-1604.3	Tht	---	---	1	---	6	3	---	Tr.	---	---
G4-1625.4	Tht	---	---	---	---	6	4	---	---	---	---
G4-1652.0	Tht	---	---	1	---	5	4	---	---	---	---
G4-1667.7	Tht	---	---	1	---	6	3	---	---	---	---
G4-1691.8	Tht	---	---	---	---	7	3	---	---	---	---
G4-1709.6	Tht	---	---	Tr.	---	5	3	---	2	---	---
G4-1738.4	Tht	---	---	2	---	5	1	---	---	---	2
G4-1759.0	Tht	---	3	1	Tr.	1	1	---	---	2	2
G4-1765.2	Tcp	---	8	2	Tr.	Tr.	---	---	---	---	---
G4-1788.9	Tcp	---	1	---	---	---	5	---	---	4	---
G4-1798.8	Tcp	---	---	1	---	---	---	---	8	1	---
G4-1995.2	Tcp	---	3	1	---	1	---	---	---	5	---
G4-2032.6	Tcp	---	---	---	---	3	---	---	6	1	---
G4-2061.2	Tcp	---	---	---	---	5	5	---	Tr.	---	---
G4-2087.9	Tcp	---	1	---	---	---	9	---	---	---	---

Table 2. Mineralogic composition of tuffs of Yucca Mountain, as estimated from X-ray diffractometer patterns of bulk samples of core—Continued

Sample No.	Stratigraphic unit	X-ray analysis (parts of ten)									
		Glass	Opal	Smectite	Mica	Clinoptilolite	Mordenite	Analcime	Alkali feldspar	Plagioclase	Quartz
Drill hole USW-G4											
G4-2117.6	Tcp	---	---	---	---	7	3	---	---	---	---
G4-2137.2	Tcp	---	---	Tr.	---	---	9	---	1	---	---
G4-2164.0	Tcp	---	---	---	---	6	4	---	---	---	---
G4-2189.3	Tcp	---	---	---	---	5	5	---	---	---	---
G4-2209.4	Tcp	---	---	1	---	4	5	---	---	---	---
G4-2239.1	Tcp	---	---	1	---	7	2	---	Tr.	---	---
G4-2252.0	Tcb	---	---	Tr.	---	8	---	---	---	---	2
G4-2709.6	Tcb	---	---	1	---	---	9	---	Tr.	---	Tr.
G4-2734.2	Tcb	---	---	---	---	Tr.	5	---	---	---	5
G4-2757.6	Tct	---	---	---	---	1	6	---	3	---	---
G4-2764.7	Tct	---	---	---	---	2	2	---	6	---	---
G4-2806.5	Tct	---	---	---	---	3	2	---	5	---	---
G4-2818.4	Tct	---	---	---	---	---	5	---	3	---	2
G4-2830.0	Tct	---	---	---	---	2	2	---	---	---	6
G4-2849.2	Tct	---	---	1	Tr.	---	---	---	---	2	7
Drill hole UE25b-1H											
UE25-2805.1	Tcb	---	---	---	---	---	3	---	2	---	5
UE25-2829.6	Tcb	---	---	---	---	---	1	---	5	---	4
UE25-2846.7	Tcb	---	---	---	---	---	4	---	4	---	2
UE25-2871.7	Tcb	---	---	---	---	---	2	---	---	---	8
UE25-2887.9	Tct	---	---	Tr.	---	---	8	---	---	---	2
UE25-2900.4	Tct	---	---	---	---	---	9	---	---	---	1

misleading, however, because the mordenite does not occur throughout the entire interval. For example, much of the Topopah Spring Member of the Paintbrush Tuff (about 170 m) and the upper part of the Prow Pass Member of the Crater Flat Tuff (about 70 m) consist of moderately to densely welded tuff that was devitrified or vapor-phase altered shortly after emplacement (Caporuscio and others, 1982). Because the original glass had already been altered prior to the zeolitization, these two parts of the "mordenite-bearing" interval consequently lack not just mordenite, but any zeolite. In drill holes USW-G1 and USW-G2, mordenite persists downward well into the upper part of the analcime zone.

Description of Mordenite

Mordenite can be readily distinguished from the commonly associated clinoptilolite by its characteristic fibrous habit that is observable in thin sections and in scanning electron micrographs. Individual mordenite fibers range in length from less than 1 to about 100 μm. The fibers are very delicate and commonly have length-to-width ratios of 20–100. The indices of refraction are difficult, if not impossible, to measure because of the fibrous nature of the mordenite and the extremely small crystal size; the mean index of refraction, however, is in the range of 1.466–1.474. The birefringence is low, about 0.003.

Mordenite in the tuffs at Yucca Mountain has three common modes of occurrence: (1) pseudomorphs of original vitric material, (2) spherulites or radial aggregates of fibers, and (3) filiform or threadlike fibers that occur singly or entwined. The pseudomorphs of original vitric particles commonly consist of a marginal film of smectite succeeded inwardly by a single layer (6–25 μm thick) of compact fibers of mordenite that grew perpendicular to the wall of the shard. Many of the pseudomorphs are hollow (figs. 4 and 5), but others have a central cavity that is filled or partly filled by a second generation of mordenite (fig. 6), clinoptilolite (figs. 5 and 7), or opal. The second-generation mordenite commonly has a higher mean index of refraction than the earlier, marginal mordenite. Spherulites of mordenite (fig. 8) are as large as 250 μm in diameter, although most are 50–100 μm in diameter. Spherulitic mordenite seems to be most common in the larger vitric particles. Filiform mordenite, which is observable only in scanning electron micrographs (figs. 9–13), occurs as delicate, straight or curved, threadlike fibers that commonly drape across or bridge earlier diagenetic minerals such as clinoptilolite (fig. 10) and opal (fig. 11) or devitrification minerals such as alkali feldspar and quartz (fig. 12). More rarely, the filiform mordenite occurs as an indescribable tangle of mostly curved fibers (fig. 13).

Figure 4. Photomicrograph of mordenite-rich tuff (sample G1-2257.2) from Bullfrog Member of the Crater Flat Tuff in drill hole USW-G1, showing well-preserved vitroclastic texture. Pseudomorphs of shards are defined by a layer of compact fibers of mordenite (M). Some pseudomorphs are hollow (H).

Figure 5. Photomicrograph of mordenite-rich tuff (sample G1-2291.1) from Bullfrog Member of the Crater Flat Tuff in drill hole USW-G1, showing well-preserved vitroclastic texture. Pseudomorphs of original vitric materials are defined by a layer of compact fibers of mordenite (M). Large pseudomorph in the central part of the photo shows relatively large, blocky crystals of clinoptilolite (C) that grew on a thin layer of compact fibers of mordenite.

Chemical Composition of Mordenite

Mordenite was separated from mordenite-rich samples of the tuffaceous beds of Calico Hills and of the Bullfrog Member of the Crater Flat Tuff by first crushing the tuffs and then disaggregating them in an ultrasonic bath. The mordenite was then concentrated by repeated gravity separations in a heavy-liquid mixture of bromoform and acetone. The final mordenite concentrates contained about 2–5 percent smectite, clinoptilolite, and hydrous iron oxide impurities.

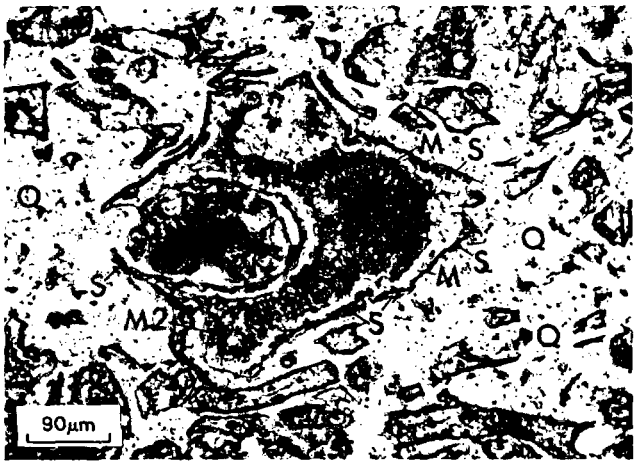

Figure 6. Photomicrograph of mordenite-bearing tuff (sample G2-3454.6) from Bullfrog Member of the Crater Flat Tuff in drill hole USW-G2, showing large pseudomorph of a vitric particle that is defined by a relatively thin layer of compact fibers of mordenite (M) followed inwardly by a second layer of coarser mordenite fibers (M2). A discontinuous film of smectite (S) outlines the pseudomorph. Matrix consists of authigenic quartz (Q).

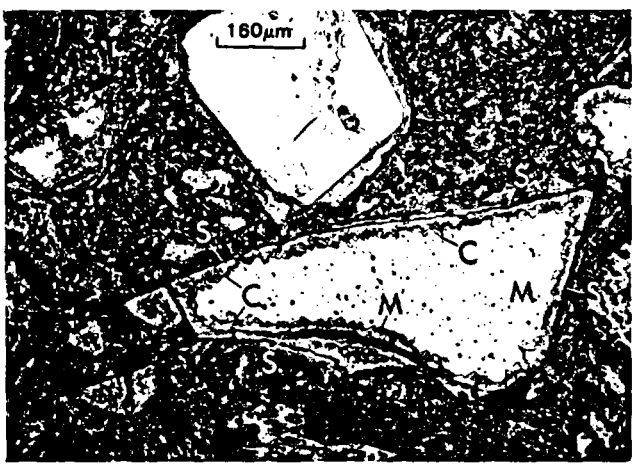

Figure 7. Photomicrograph of mordenite-bearing tuff (sample G2-2029.7) from the tuffaceous beds of Calico Hills in drill hole USW-G2, showing a hollow pseudomorph of a relatively large vitric particle. From margin to center, the pseudomorph consists of a discontinuous film of smectite (S), a thin layer of compact fibers of mordenite (M), and blocky crystals of clinoptilolite (C) that project into the hollow interior.

Figure 8. Photomicrograph of mordenite-bearing tuff (sample G2-3454.6) from Bullfrog Member of the Crater Flat Tuff in drill hole USW-G2, showing spherulitic mordenite. Crossed nicols.

Figure 9. Scanning electron micrograph of sample UE25-2900.4 from the tuffaceous beds of Calico Hills in drill hole UE25b-1H, showing compact layer of filiform mordenite that projects into the hollow interior of a pseudomorph of a shard.

The chemical analyses by X-ray fluorescence and the contents of the unit cell based on 96 oxygen atoms are given in table 3. Both mordenites that were sampled are siliceous; the Si:Al ratios are 4.78 and 5.06. Monovalent cations exceed divalent ones for both samples. The Na:K ratio for the mordenite from the tuffaceous beds of Calico Hills is about 0.57, but the Na:K ratio for mordenite from the Bullfrog Member of the Crater Flat Tuff is about 2.19. The potassium content is unusually high (Passaglia, 1975) in both samples, but especially so in the mordenite from the tuffaceous beds of Calico Hills where potassium represents about 41 percent of the exchangeable cations.

Electron microprobe analyses of other mordenite-bearing samples were attempted without much success. All the electron microprobe analyses have low totals, and the analyzed content of sodium seems especially low. The electron microprobe analyses do suggest, however, a range of Si:Al ratios of about 4.8-5.2. Three electron microprobe analyses of mordenite from the Prow Pass Member of the Crater Flat Tuff, reported by Caporuscio and others (1982, p. 90), show that the Si:Al ratio is

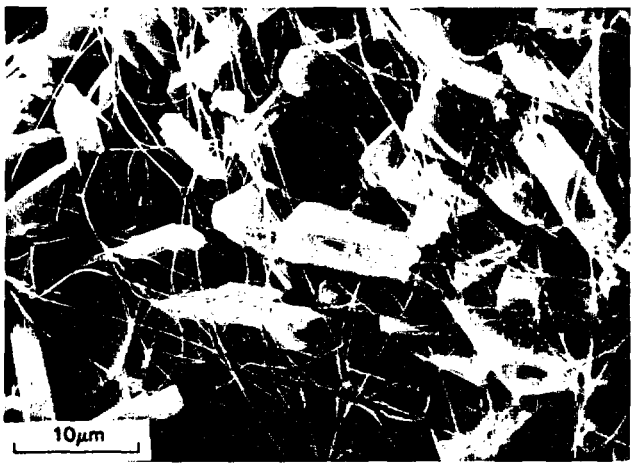

Figure 10. Scanning electron micrograph of sample G2-2029.7 from the tuffaceous beds of Calico Hills in drill hole USW-G2, showing filiform mordenite draped across euhedral clinoptilolite.

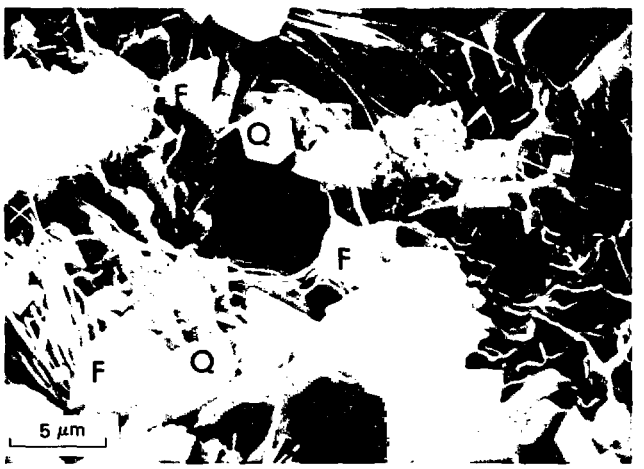

Figure 12. Scanning electron micrograph of sample G2-3454.6 from Bullfrog Member of the Crater Flat Tuff in drill hole USW-G2, showing filiform mordenite draped across authigenic alkali feldspar (F) and quartz (Q).

Figure 11. Scanning electron micrograph of sample G2-2029.7 from the tuffaceous beds of Calico Hills in drill hole USW-G2, showing a tangle of filiform mordenite draped across lepispheres of opal.

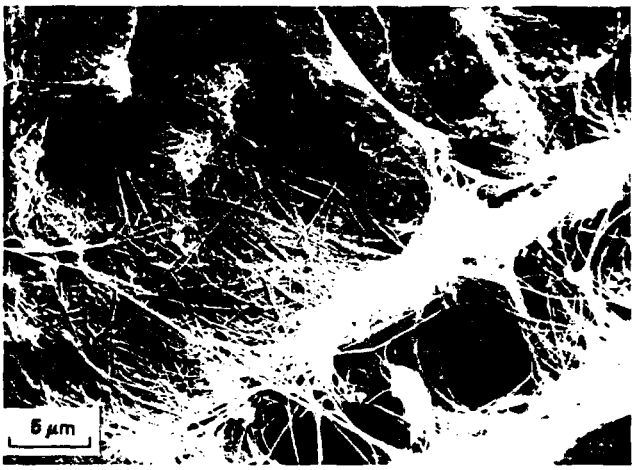

Figure 13. Scanning electron micrograph of sample G1-2291.1 from Bullfrog Member of the Crater Flat Tuff in drill hole USW-G1, showing a tangle of filiform mordenite in a pseudomorph of a pumice fragment.

4.86–5.11 and that sodium is greatly in excess of the other exchangeable cations.

Thus, mordenite from the tuffs of Yucca Mountain has a range in Si:Al ratios of about 4.8–5.2 and is alkali rich. Some mordenite is potassic, but the stratigraphic or diagenetic significance of such is unknown.

X-ray Powder Diffraction Data for Mordenite

An indexed powder pattern for mordenite from the Bullfrog Member of the Crater Flat Tuff is given in table 4, and cell parameters for five mordenites from the tuffaceous beds of Calico Hills and the Crater Flat Tuff are given in table 5. The cell parameters show the following ranges: $a=18.074$–18.114 Å, $b=20.435$–20.528 Å, $c=7.489$–7.546 Å, and $V=2{,}771$–$2{,}803$ Å^3. Except for slightly smaller and slightly larger c dimensions, these ranges for the Yucca Mountain mordenites are within the ranges reported by Passaglia (1975) for 35 mordenites from a variety of rock types and localities.

Passaglia's (1975) crystal chemical study of mordenites demonstrated a negative correlation between the b dimension and the $Si:Si+Al+Fe^{3+}$ ratio, such that the $Si:Si+Al+Fe^{3+}\pm0.0113=8.12391-0.35632\,b$. The two analyzed samples (G1-2291.1 and G2-1996.6) from Yucca Mountain confirm this relationship. The $Si:Si+Al+Fe^{3+}$ ratio for sample G1-2291.1 from the

Table 3. Chemical analyses and composition of unit cell of mordenite from Yucca Mountain, Nevada

	G1-2291.1[1]	G2-1996.6[2]
Chemical analyses [Analyses by x-ray fluorescence by A.J. Bartel. H_2O determined by loss on ignition at 900 °C]		
SiO_2	68.2	68.6
Al_2O_3	12.1	11.5
Fe_2O_3	0.92	0.67
MgO	0.13	0.44
CaO	2.02	2.54
Na_2O	3.24	1.18
K_2O	2.26	3.16
TiO_2	0.08	0.05
P_2O_5	<0.05	<0.05
MnO	0.09	0.03
H_2O	10.8	11.5
Total	99.84	99.67
Composition of unit cell [Calculated on the basis of 96 oxygen atoms]		
Si	39.50	39.96
Al	8.26	7.90
Fe^{3+}	0.40	0.30
Mg	0.12	0.38
Ca	1.26	1.58
Na	3.64	1.34
K	1.66	2.34
H_2O	20.86	22.34
Si:Al	4.78	5.06

[1]G1-2291.1--Lab. No. D260299; separated from the Bullfrog Member of the Crater Flat Tuff in drill hole USW-G1.

[2]G2-1996.6--Lab. No. D260303; separated from the tuffaceous beds of Calico Hills in drill hole USW-G2.

chemical analysis (table 3) is 0.82, and by calculation from the *b* dimension is 0.81 ± 0.01. The $Si:Si+Al+Fe^{3+}$ ratio for sample G2-1996.6 from the chemical analysis is 0.83 and by calculation from *b* is 0.83 ± 0.01. Inasmuch as two mordenites in table 5 have a *b* dimension smaller than that for sample G2-1996.6, these mordenites probably are more siliceous than sample G2-1996.6.

Paragenesis

The relative age relationships of the diagenetic silicate minerals in the tuffs can be determined by the

Table 4. X-ray powder diffraction data for mordenite from Yucca Mountain, Nevada

[Sample No. G1-2291.1 from Bullfrog Member of the Crater Flat Tuff in drill hole USW-G1. Chemical analysis for sample given in table 3]

hkl	d_{calc}(A)	d_{obs}(A)	I
110	13.57	13.60	2
020	10.26	10.06	15
200	9.05	9.03	72
111	6.60	6.61	35
130	6.40	6.41	14
021	6.08	6.09	3
310	5.79	5.81	8
131	4.88		
311	4.59		
330	4.53	4.54	26
240	4.46		
420	4.14	4.15	9
150	4.004	3.991	58
241	3.842	3.841	12
002	3.773	3.771	2
421	3.629	3.628	3
510	3.564	3.559	4
022	3.541		
202	3.482	3.479	100
060	3.421		
350	3.394	3.395	40
222	3.298		
511	3.223	3.229	77
530	3.199	3.194	47
312	3.161		
061	3.116		
441	3.095		
042	3.040		
600	3.016		
261	2.946		
402, 332	2.898	2.897	27
152	2.746		
550	2.715		
171	2.702	2.702	2
370	2.637	2.626	1
512	2.590	2.589	7
080	2.566	2.567	7
352	2.523	2.523	17
641	2.458		
532	2.440		
262	2.441		
622	2.296		
570	2.279		
800	2.262	2.261	2
480	2.232		
661	2.167	2.168	4
082	2.122	2.123	2
0·10·0	2.053	2.053	3
732	2.036	2.037	3
443	2.021		
841	1.996	1.995	2

Table 5. Cell parameters for mordenite from Yucca Mountain, Nevada

Sample No.	a(Å)	b(Å)	c(Å)	V(Å^3)
G1-2291.1[1]	18.096(8)	20.528(9)	7.546(6)	2803(2)
G2-1996.6[2]	18.074(27)	20.470(31)	7.489(13)	2771(6)
G4-2137.2[3]	18.095(12)	20.435(13)	7.527(6)	2783(2)
G4-2709.6[4]	18.087(15)	20.439(10)	7.521(5)	2780(3)
UE25-2900.4[5]	18.114(22)	20.497(17)	7.521(8)	2792(4)

[1]G1-2291.1--Bullfrog Member of the Crater Flat Tuff in drill hole USW-G1.

[2]G2-1996.6--Tuffaceous beds of Calico Hills in drill hole USW-G2.

[3]G4-2137.2--Prow Pass Member of the Crater Flat Tuff in drill hole USW-G4.

[4]G4-2709.6--Bullfrog Member of the Crater Flat Tuff in drill hole USW-G4.

[5]UE25-2900.4--Tram Member of the Crater Flat Tuff in drill hole UE25b-1H.

sequence of filling of voids and once-hollow pseudomorphs of vitric particles and by replacement relations. The mineral in the interior of a void or pseudomorph presumably formed later than the mineral(s) nearer the periphery. The following sequences of crystallization involving mordenite were compiled from thin-section examination and scanning electron microscopy:

Paragenesis of diagenetic silicate minerals
[Earliest mineral listed on left]

Smectite - clinoptilolite - mordenite
Smectite - mordenite - clinoptilolite
Smectite - mordenite - clinoptilolite - mordenite
Smectite - mordenite - clinoptilolite - opal
Smectite - mordenite - quartz
Mordenite - clinoptilolite - analcime + quartz
Smectite - mordenite - analcime + quartz

These relationships indicate that smectite was consistently the earliest mineral to form and that mordenite was commonly the earliest zeolite to crystallize in the mordenite-bearing tuffs.

Scanning electron micrographs of the tuffs that contain clinoptilolite and mordenite commonly show that filiform mordenite postdates the clinoptilolite (fig. 10). Unlike the clinoptilolite shown in figure 10, some clinoptilolite was affected by dissolution prior to the crystallization of the filiform mordenite as clearly indicated by the scanning electron micrographs in figures 14 and 15. Figure 14 is a micrograph from the tuffaceous beds of Calico Hills in drill hole USW-G2 and shows filiform mordenite draped on clinoptilolite that had been etched before the crystallization of the mordenite. More severe dissolution of clinoptilolite is evident in the figure 15 micrographs from the Bullfrog Member of the Crater Flat Tuff in drill hole USW-G1. Figure 15*A* shows a large clinoptilolite crystal, similar to that illustrated in figure 5, that grew on a mat of compact fibers of mordenite. The clinoptilolite has obviously been affected by dissolution, and minute filiform crystals of mordenite grew on the dissolution surface (fig. 15*B*). Neither the dissolution of the clinoptilolite nor the second generation of mordenite could be seen in thin sections of the same sample. Similar dissolution of clinoptilolite followed by crystallization of filiform mordenite has also been recognized in the Pah Canyon Member of the Paintbrush Tuff in drill hole USW-G2.

Thus, evidence from the study of thin sections and scanning electron micrographs indicates two generations of mordenite in some tuffs at Yucca Mountain. At least locally, the second generation of filiform mordenite crystallized after the associated clinoptilolite had been affected by dissolution.

CHEMICAL CHANGES DURING ZEOLITIZATION

Chemical analyses of bulk samples of mordenite-rich tuff from tuffaceous beds of Calico Hills and the Crater Flat Tuff are given in table 6, along with a chemical analysis of fresh glass from the Topopah Spring Member of the Paintbrush Tuff. In addition to the obvious and significant increase in the H_2O content of the mordenite-rich tuffs, other approximate changes in chemical composition from fresh glass to zeolitic tuff were inferred by assuming that the Al_2O_3 content remained constant during diagenetic alteration, although this assumption has not been rigorously tested. Gains and losses of chemical components are based on the

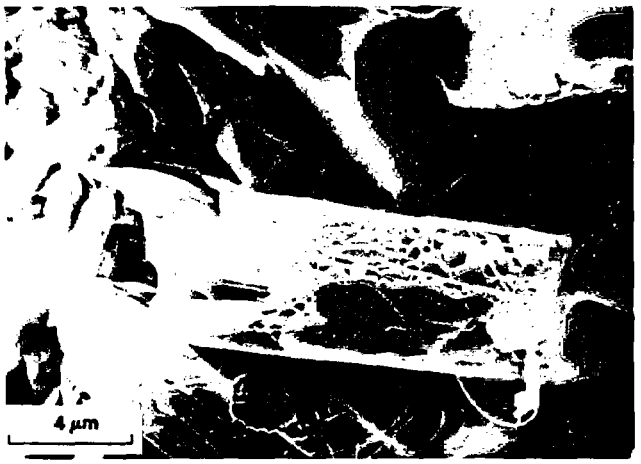

Figure 14. Scanning electron micrograph of sample G2-2072.9 from the tuffaceous beds of Calico Hills in drill hole USW-G2, showing filiform mordenite draped on clinoptilolite that had been etched prior to the crystallization of the mordenite.

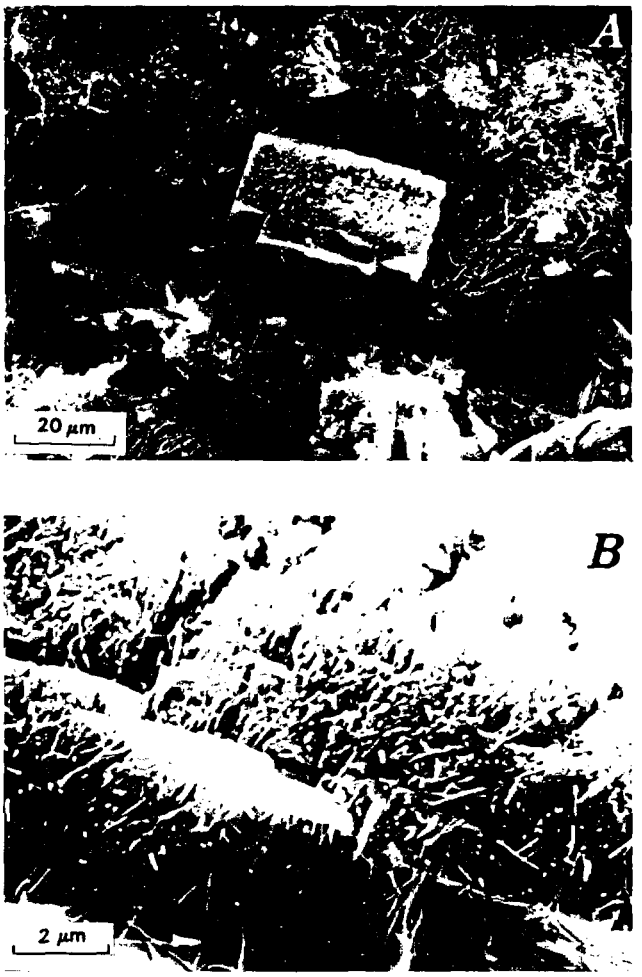

Figure 15. Scanning electron micrographs of sample G1-2291.1 from the Bullfrog Member of the Crater Flat Tuff in drill hole USW-G1. *A*, Large, blocky crystal of clinoptilolite that grew on a mat of compact filiform mordenite. Clinoptilolite shows obvious effects of dissolution. *B*, Close-up of clinoptilolite showing minute crystals of filiform mordenite that grew from the dissolution surface of the clinoptilolite.

assumption that the original composition of the mordenite-rich tuff was similar to the composition of the glass from the Topopah Spring Member. Numerous analyses of glass by Vaniman and others (1984) from the various stratigraphic units at Yucca Mountain indicate that this is a valid assumption. The chemical gains and losses for the mordenite-rich tuffs given in table 6 were determined by (1) recalculation of all the analyses to the anhydrous form and normalizing to 100 percent, (2) then, recalculation of these normalized analyses of the zeolitic tuffs, assuming constant Al_2O_3 content of the fresh glass, and (3) finally, comparison of the Al_2O_3-constant analyses with the anhydrous analysis of the fresh glass.

The mordenite-rich tuffs differ significantly in composition from the fresh glass. Relative to the unaltered glass, all the mordenite-rich tuffs show consistent gains of MgO and CaO and losses of Na_2O, K_2O, and SiO_2. Most mordenite-rich tuff has also gained Fe_2O_3. The most obvious chemical changes in the mordenite-rich tuffs are the gains of alkaline earth elements, particularly calcium, and the losses of alkalis. Similar gains and losses have been noted for the diagenetic alteration of silicic glass to mainly clinoptilolite in the John Day Formation of Oregon (Hay, 1963) and the Ricardo Formation of California (Sheppard and Gude, 1965).

GENESIS OF MORDENITE

Previous studies by others indicated that the formation of zeolites and associated silicate minerals in the tuffs at Yucca Mountain and adjacent areas and the vertical arrangement of the diagenetic zones are due to the alteration of silicic glass in a ground-water system. Hoover (1968) attributed the diagenetic mineral zonation to differences in the chemistry of the pore water, but more recent investigators (Moncure and others, 1981; Bish and others, 1982; Caporuscio and others, 1982) have explained the zonation by a regime of changing pore-water chemistry during diagenesis in conjunction with increased burial and higher temperatures.

The initial chemistry of the ground water and, hence, the pore water, was modified greatly by dissolution of the highly soluble silicic glass in the tuffs. Continued dissolution of the glass elevated the salinity and pH of the pore water and provided a favorable chemical environment for the crystallization of zeolites in the clinoptilolite-mordenite zone. Dissolution of the silicic

Table 6. Chemical analyses and chemical comparison of unaltered glass and mordenite-rich tuffs from Yucca Mountain, Nevada

[Analyses by X-ray fluorescence by A.J. Bartel, K.C. Stewart, and J.E. Taggart. H_2O determined by loss on ignition at 900 °C. A, uncorrected analysis in weight percent; B, analysis recalculated to anhydrous and normalized to 100 percent; C, gains (+) and losses (−) in weight percent assuming the constant Al_2O_3 value of the unaltered glass (analysis 1B)]

	1		2			3			4			5			6		
	A	B	A	B	C	A	B	C	A	B	C	A	B	C	A	B	C
SiO_2	74.8	77.70	69.2	77.80	-3.96	67.6	75.62	-9.77	68.0	75.47	-10.45	68.1	76.41	-7.54	67.9	74.57	-12.66
Al_2O_3	11.9	12.36	11.6	13.04	---	12.3	13.76	---	12.5	13.87	---	12.0	13.46	---	12.9	14.17	---
Fe_2O_3	0.80	0.83	0.71	0.80	-0.03	1.22	1.36	+0.39	1.21	1.34	+0.36	1.20	1.35	+0.41	1.48	1.62	+0.58
MgO	<0.10	---	0.39	0.44	+0.44	0.13	0.14	+0.13	0.15	0.17	+0.17	0.13	0.15	+0.14	0.38	0.42	+0.37
CaO	0.50	0.52	2.46	2.76	+2.74	2.49	2.78	+1.98	2.04	2.26	+1.49	2.75	3.08	+2.31	2.35	2.58	+1.73
Na_2O	3.31	3.44	1.21	1.36	-2.15	2.32	2.60	-1.10	3.40	3.77	-0.08	2.78	3.12	-0.58	2.18	2.39	-1.36
K_2O	4.83	5.02	3.24	3.64	-1.57	3.22	3.60	-1.79	2.38	2.64	-2.67	2.02	2.27	-2.94	3.57	3.92	-1.60
TiO_2	0.07	0.07	0.06	0.07	0.00	0.11	0.12	+0.04	0.12	0.13	+0.05	0.12	0.13	+0.05	0.19	0.21	+0.11
P_2O_5	<0.05	---	<0.05	---	0.00	<0.05	---	0.00	<0.05	---	0.00	<0.05	---	0.00	0.05	0.05	+0.04
MnO	0.06	0.06	0.07	0.08	+0.02	<0.02	---	-0.06	0.30	0.33	+0.23	0.02	0.02	-0.04	0.05	0.05	-0.02
H_2O	3.49	---	11.0	---	---	9.70	---	---	9.62	---	---	10.6	---	---	8.46	---	---
Total	99.76	100.00	99.94	99.99	---	99.09	99.98	---	99.72	99.98	---	99.72	99.99	---	99.51	99.98	---

1. Unaltered glass; sample No. G1-1307.7; separated from the Topopah Spring Member of the Paintbrush Tuff from drill hole USW-G1.
2. Mordenite-rich tuff; sample No. G2-1996.6; bulk sample of the tuffaceous beds of Calico Hills from drill hole USW-G2.
3. Mordenite-rich tuff; sample No. G4-2137.2; bulk sample of the Prow Pass Member of the Crater Flat Tuff from drill hole USW-G4.
4. Mordenite-rich tuff; sample No. G1-2291.1; bulk sample of the Bullfrog Member of the Crater Flat Tuff from drill hole USW-G1.
5. Mordenite-rich tuff; sample No. G4-2709.6; bulk sample of the Bullfrog Member of the Crater Flat Tuff from drill hole USW-G4.
6. Mordenite-rich tuff; sample No. UE25-2900.4; bulk sample of the Tram Member of the Crater Flat Tuff from drill hole UE25b-1H.

glass certainly enriched the pore water in alkalis and silica. Inasmuch as the original compositions of the glass from the various stratigraphic units at Yucca Mountain are similar, the original glass composition probably played no role in the arrangement of the diagenetic zones or in the composition of the individual diagenetic minerals. The highly silicic composition of the original glass did, however, dictate the ultimate crystallization of the highly siliceous zeolites, clinoptilolite and mordenite. Mariner and Surdam (1970) showed experimentally that the pH of the pore water also influences the Si:Al ratio of the pore water and the Si:Al ratio of the zeolite precipitate. A pH in the range of 7–9 would probably favor crystallization of siliceous zeolites such as clinoptilolite or mordenite rather than an aluminous zeolite such as phillipsite. Experiments with natural silicic glasses led Phillips (1983) to conclude that mordenite is generally favored by mildly alkaline solutions.

Much of the mordenite in the clinoptilolite-mordenite zone at Yucca Mountain is a direct alteration product of the silicic glass, and dissolution of the glass provided the essential components for this mordenite. Petrographic evidence indicates that at least some of the pseudomorphs of vitric particles formed by crystallization of mordenite in cavities from which the glass had been dissolved. The still-hollow pseudomorphs (figs. 4, 5, and 7) are difficult to explain in any other way. Other mordenite replacements probably were contemporaneous with dissolution of the glass, but convincing evidence is lacking. As suggested by some of the scanning electron micrographs (figs. 14 and 15), some relatively late mordenite postdates dissolution of clinoptilolite, and the chemical components for this mordenite may have been derived from the clinoptilolite.

The following brief summary of the synthesis of mordenite provides a foundation for a discussion of the crystallization of mordenite versus clinoptilolite. Mordenite was apparently first synthesized by Barrer (1948), who established that this zeolite readily crystallized from sodium aluminosilicate gels in the temperature range of 265–295 °C. Since then, Barrer and other investigators synthesized mordenite from a variety of starting materials and chemical systems and over a temperature range of about 75–400 °C (Senderov, 1963; Seki, 1973; Barrer, 1982). The first mordenite synthesis from natural glass was accomplished by Ellis (1960) using powdered silicic obsidian that was suspended in the natural hydrothermal fluid of a bore hole at Wairakei, New Zealand. More recently, laboratory syntheses of mordenite from natural silicic glasses have been reported by Wirsching (1976), Hawkins and others (1978), Kirov and others (1979), and Phillips (1983). These experimental studies indicated that mordenite is favored over clinoptilolite by higher temperatures and higher Na:K ratios of the system. Using natural clinoptilolite as a starting material in a sodium system, Kusakabe and others (1981) found that clinoptilolite reacted to form mordenite under conditions of increased temperature, pH, and (or) Na^+ concentration, as shown schematically in figure 16. The hydrothermal conversion of clinoptilolite to mordenite was accomplished by Kusakabe and others (1981) over ranges of temperature of 170–365 °C, pHs of 5.3–12.23, and Na^+ concentrations of 40–2,300 ppm. The conversion to mordenite shifted to relatively higher temperatures with a decrease in Na^+ concentration or pH.

We have no direct evidence as to which of the above factors evaluated by Kusakabe and others (1981) may have caused the conversion of clinoptilolite to mordenite in the tuffs of Yucca Mountain, but some circumstantial evidence points to elevated temperatures. Drill hole USW-G2, the northernmost hole studied, is only about 8 km south of the Timber Mountain caldera, which postdates all the stratigraphic units penetrated by the drill holes. Compared to the tuffs in the other drill holes we studied, tuffs in USW-G2 show certain effects suggestive of exposure to higher temperatures. All the boundaries between the diagenetic zones rise in elevation from south to north (toward the Timber Mountain caldera), especially from drill hole USW-G1 to USW-G2 (fig. 3). In addition, the analcime zone is significantly thinner in USW-G2 than in USW-G1. The increase in the amount of interstratified illite in authigenic illite/smectite with depth and the occurrence of illite in the lower part of USW-G2 are suggestive of higher temperatures (180–230 °C) in USW-G2 than in USW-G1 (Caporuscio and others, 1982). The thickness of the mordenite-bearing interval is greater in USW-G2 than in any of the other drill holes to the south. In fact, mordenite occurs only rarely in the Bullfrog and Tram Members of the Crater Flat Tuff in drill hole USW-G3 (Vaniman and others, 1984), about 8 km south of USW-G2, and has not been reported at all in drill hole J-13 (Heiken and Bevier, 1979), about 11 km southeast of USW-G2. Finally, minerals characteristic of hydrothermal alteration, such as barite, fluorite, pyrite, and epidote, occur in parts of the Crater Flat Tuff and in stratigraphically lower units in drill hole USW-G2 (Caporuscio and others, 1982; Maldonado and Koether, 1983).

Corroborative data relating to the role of temperature in the conversion of clinoptilolite to mordenite are provided by hydrothermal experiments that were designed to simulate repository conditions for high-level nuclear waste (Blacic and others, 1982). Samples of clinoptilolite-rich tuff from Yucca Mountain showed the reaction of clinoptilolite to form mordenite after prolonged hydrothermal exposure at 120 and 180 °C (Bish and others, 1982).

Mineralogical studies of silicic volcanic rocks from other areas also seem to show a relationship between temperature and the distribution of clinoptilolite and

mordenite. Drill hole Y-6 in Yellowstone National Park, Wyo. (Bargar and Beeson, 1984), penetrated the Pleistocene Plateau Rhyolite which has a variety of hydrothermal minerals along fractures and in cavities. Clinoptilolite occurs only in the upper 30 m of the core, but mordenite persists to a depth of about 130 m where a temperature of about 170 °C was measured. Surdam (1985) studied the alteration of rhyolitic tuffs in the Miocene Obispo Formation of California and noted that the distribution of clinoptilolite and mordenite is related to the proximity of intrusive bodies. Mordenite occurs in the tuffs closest to the intrusives (higher temperature), and clinoptilolite occurs more distant from the intrusives (lower temperature).

Thus, at least some of the mordenite in the silicic tuffs beneath Yucca Mountain seems due to diagenesis in a relatively high thermal regime near the Timber Mountain caldera to the north. This conclusion does not, however, mitigate the importance of the pore-water chemistry during diagenesis of the tuffs.

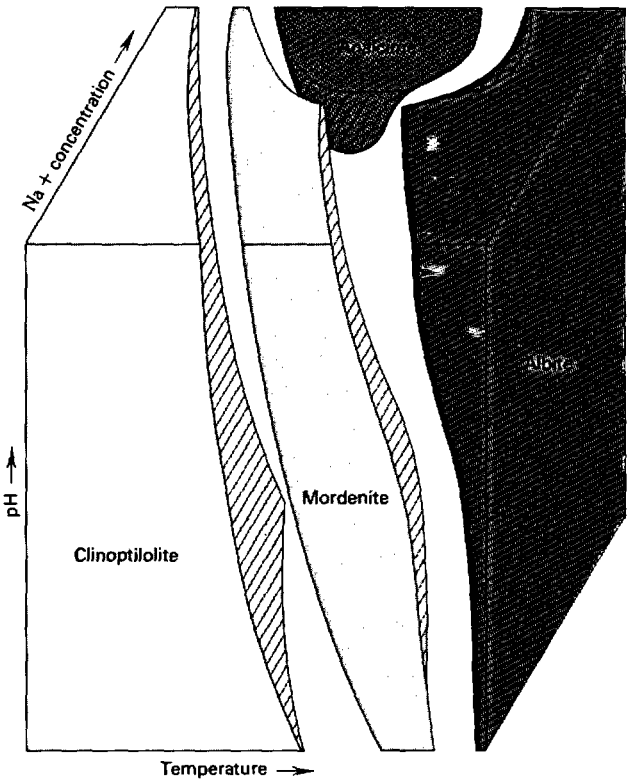

Figure 16. Schematic diagram showing relationships of clinoptilolite, mordenite, analcime, and albite as functions of temperature, pH, and sodium ion concentration, from Kusakabe and others (1981).

REFERENCES CITED

Appleman, D.E., and Evans, H.T., Jr., 1973, Job 9214: Indexing and least squares refinement of powder diffraction data: U.S. Department of Commerce, NTIS Document PB-216188, 26 p.

Bargar, K.E., and Beeson, M.H., 1984, Hydrothermal alteration in research drill hole Y-6, Upper Firehole River, Yellowstone National Park, Wyoming: U.S. Geological Survey Professional Paper 1054-B, 24 p.

Barrer, R.M., 1948, Syntheses and reactions of mordenite: Journal of the Chemical Society (London), p. 2158-2163.

_____1982, Hydrothermal chemistry of zeolites: London, Academic Press, 360 p.

Bish, D.L., 1981, Detailed mineralogical characterization of the Bullfrog and Tram Members in USW-G1, with emphasis on clay mineralogy: Los Alamos National Laboratory Report LA-9021-MS, 21 p.

Bish, D.L., Caporuscio, F.A., Copp, J.F., Crowe, B.M., Purson, J.D., Smyth, J.R., and Warren, R.G., 1981, Preliminary stratigraphic and petrologic characterization of core samples from USW-G1, Yucca Mountain, Nevada: Los Alamos National Laboratory Report LA-8840-MS, 66 p.

Bish, D.L., Vaniman, D.T., Byers, F.M., Jr., and Broxton, D.E., 1982, Summary of the mineralogy-petrology of tuffs of Yucca Mountain and the secondary-phase thermal stability in tuffs: Los Alamos National Laboratory Report LA-9321-MS, 47 p.

Blacic, J.D., Bish, D.L., and Gooley, R., 1982, Physical property and mineralogical changes in tuff exposed to simulated high-level nuclear waste repository conditions: Geological Society of America Abstracts with Programs, v. 14, no. 6, p. 303.

Byers, F.M., Jr., Carr, W.J., Christiansen, R.L., Lipman, P.W., Orkild, P.P., and Quinlivan, W.D., 1976, Geologic map of the Timber Mountain caldera area, Nye County, Nevada: U.S. Geological Survey Miscellaneous Investigations Map I-891, scale 1:48,000, 1 sheet, 10 p.

Byers, F.M., Jr., Carr, W.J., Orkild, P.P., Quinlivan, W.D., and Sargent, K.A., 1976, Volcanic suites and related cauldrons of Timber Mountain-Oasis Valley caldera complex, southern Nevada: U.S. Geological Survey Professional Paper 919, 70 p.

Caporuscio, F.A., Vaniman, D.T., Bish, D.L., Broxton, D.E., Arney, B., Heiken, G.H., Byers, F.M., Jr., Gooley, R., and Semarge, E., 1982, Petrologic studies of drill cores USW-G2 and UE25b-1H, Yucca Mountain, Nevada: Los Alamos National Laboratory Report LA-9255-MS, 111 p.

Carlos, B.A., 1985, Minerals in fractures of the unsaturated zone from drill core USW-G-4, Yucca Mountain, Nye County, Nevada: Los Alamos National Laboratory Report LA-10415-MS, 55 p.

Carr, W.J., 1982, Volcano-tectonic history of Crater Flat, southwestern Nevada, as suggested by new evidence from drill hole USW-VH-1 and vicinity: U.S. Geological Survey Open-File Report 82-457, 23 p.

Christiansen, R.L., and Lipman, P.W., 1965, Geologic map of the Topopah Spring NW quadrangle, Nye County, Nevada: U.S. Geological Survey Geologic Quadrangle Map GQ-444, scale 1:24,000.

Christiansen, R.L., Lipman, P.W., Carr, W.J., Byers, F.M., Jr., Orkild, P.P., and Sargent, K.A., 1977, Timber Mountain-Oasis Valley caldera complex of southern Nevada: Geological Society of America Bulletin, v. 88, p. 943-959.

Ellis, A.J., 1960, Mordenite synthesis in a natural hydrothermal solution: Geochimica et Cosmochimica Acta, v. 19, p. 145-146.

Hawkins, D.B., Sheppard, R.A., and Gude A.J., 3d, 1978, Hydrothermal synthesis of clinoptilolite and comments on the assemblage phillipsite - clinoptilolite - mordenite, *in* Sand, L.B., and Mumpton, F.A., eds., Natural zeolites; occurrence, properties, use: Elmsford, N.Y., Pergamon Press, p. 337-343.

Hay, R.L., 1963, Stratigraphy and zeolitic diagenesis of the John Day Formation of Oregon: University of California Publications in Geological Sciences, v. 42, no. 5, p. 199-262.

Heiken, G.H., and Bevier, M.L., 1979, Petrology of tuff units from the J-13 drill site, Jackass Flats, Nevada: Los Alamos National Laboratory Report LA-7563-MS, 55 p.

Hoover, D.L., 1968, Genesis of zeolites, Nevada Test Site, *in* Eckel, E.B., ed., Nevada Test Site: Geological Society of America Memoir 110, p. 275-284.

Iijima, Azuma, 1978, Geological occurrences of zeolite in marine environments, *in* Sand, L.B., and Mumpton, F.A., eds., Natural zeolites; occurrence, properties, use: Elmsford, N.Y., Pergamon Press, p. 175-198.

Kirov, G.N., Pechigargov, V., and Landzheva, E., 1979, Experimental crystallization of volcanic glasses in a thermal gradient field: Chemical Geology, v. 26, p. 17-28.

Kusakabe, Hirotatsu, Minato, Hideo, Utada, Minoru, and Yamanaka, Takamitsu, 1981, Phase relations of clinoptilolite, mordenite, analcime, and albite with increasing pH, sodium ion concentration, and temperature: University of Tokyo Scientific Papers of the College of General Education, v. 31, no. 1, p. 39-59.

Lipman, P.W., and McKay, E.J., 1965, Geologic map of the Topopah Spring SW quadrangle, Nye County, Nevada: U.S. Geological Survey Geologic Quadrangle Map GQ-439, scale 1:24,000.

Maldonado, Florian, and Koether, S.L., 1983, Stratigraphy, structure, and some petrographic features of Tertiary volcanic rocks of the USW-G2 drill hole, Yucca Mountain, Nye County, Nevada: U.S. Geological Survey Open-File Report 83-732, 83 p.

Mariner, R.H., and Surdam, R.C., 1970, Alkalinity and formation of zeolites in saline alkaline lakes: Science, v. 170, p. 977-980.

Moncure, G.K., Surdam, R.C., and McKague, H.L., 1981, Zeolite diagenesis below Pahute Mesa, Nevada Test Site: Clays and Clay Minerals, v. 29, p. 385-396.

Passaglia, Elio, 1975, The crystal chemistry of mordenites: Contributions to Mineralogy and Petrology, v. 50, p. 65-77.

Phillips, L.V., 1983, Mordenite occurrences in the Marysvale area, Piute County, Utah: A field and experimental study: Brigham Young University Geology Studies, v. 30, pt. 1, p. 95-111.

Scott, R.B., and Costellanos, Mayra, 1984, Stratigraphic and structural relations of volcanic rocks in drill holes USW GU-3 and USW G-3, Yucca Mountain, Nye County, Nevada: U.S. Geological Survey Open-File Report 84-491, 121 p.

Seki, Yotaro, 1973, Ionic substitution and stability of mordenite: Geological Society of Japan Journal, v. 79, no. 10, p. 669-676.

Senderov, E.E., 1963, Crystallization of mordenite under hydrothermal conditions: Geochemistry, no. 9, p. 848-859.

Sheppard, R.A., and Gude, A.J., 3d, 1965, Zeolitic authigenesis of tuffs in the Ricardo Formation, Kern County, southern California, *in* Geological Survey research 1965: U.S. Geological Survey Professional Paper 525-D, p. D44-D47.

_____1968, Distribution and genesis of authigenic silicate minerals in tuffs of Pleistocene Lake Tecopa, Inyo County, California: U.S. Geological Survey Professional Paper 597, 38 p.

Spengler, R.W., Byers, F.M., Jr., and Warner, J.B., 1981, Stratigraphy and structure of volcanic rocks in drill hole USW-G1, Yucca Mountain, Nye County, Nevada: U.S. Geological Survey Open-File Report 81-1349, 50 p.

Spengler, R.W., and Chornack, M.P., 1984, Stratigraphic and structural characteristics of volcanic rocks in core hole USW G-4, Yucca Mountain, Nye County, Nevada: U.S. Geological Survey Open-File Report 84-789, 82 p.

Spengler, R.W., Muller, D.C., and Livermore, R.B., 1979, Preliminary report on the geology and geophysics of drill hole UE25a-1, Yucca Mountain, Nevada Test Site: U.S. Geological Survey Open-File Report 79-1244, 43 p.

Surdam, R.C., 1985, Diagenesis of the Miocene Obispo Formation, Coast Range, California, *in* Volume of Abstracts: International Conference on the occurrence, properties, and utilization of natural zeolites, Budapest, Hungary, August 12-16, 1985, p. 10-11.

Sykes, M.L., Heiken, G.H., and Smyth, J.R., 1979, Mineralogy and petrology of tuff units from the UE25a-1 drill site, Yucca Mountain, Nevada: Los Alamos National Laboratory Report LA-8139-MS, 76 p.

Vaniman, D.T., Bish, D.L., Broxton, D.E., Byers, F.M., Jr., Heiken, G.H., Carlos, B.A., Semarge, E., Caporuscio, F.A., and Gooley, R., 1984, Variations in authigenic mineralogy and sorptive zeolite abundance at Yucca Mountain, Nevada, based on studies of drill cores USW GU-3 and G-3: Los Alamos National Laboratory Report LA-9707-MS, 71 p.

Wirsching, Ulrike, 1976, Experiments on hydrothermal alteration processes of rhyolitic glass in closed and "open" system: Neues Jahrbuch für Mineralogie - Monatshefte, v. 5, p. 203-213.

U.S. GOVERNMENT PRINTING OFFICE: 1988—573-047/66,072 REGION NO. 8